



Comparison of Al¹⁸F- and ⁶⁸Ga-labeled NOTA-PEG₄-LLP2A for PET imaging of very late antigen-4 in melanoma

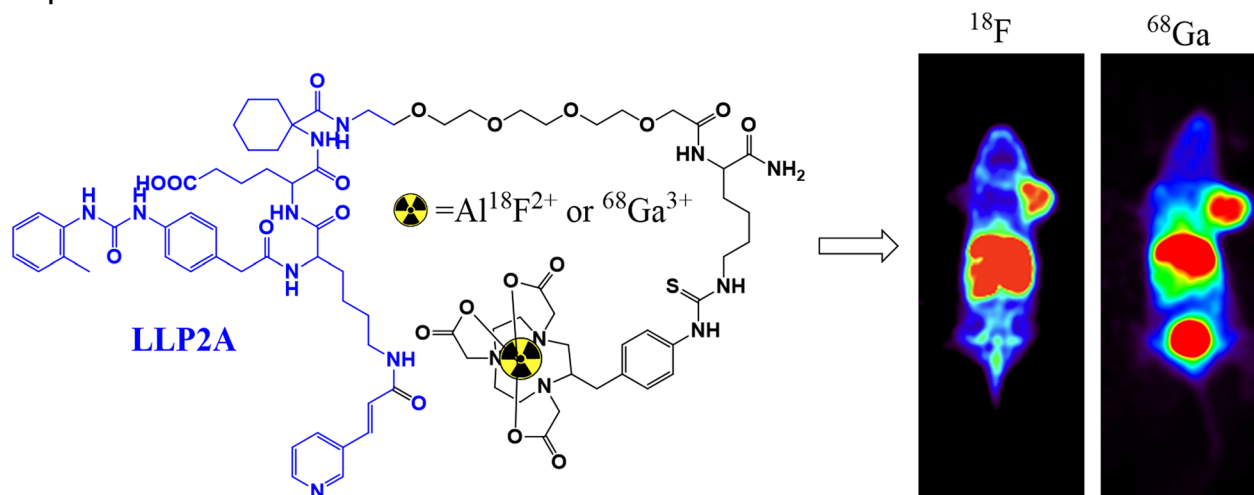
Yongkang Gai^{1,2} · Lujie Yuan^{1,2} · Lingyi Sun³ · Huiling Li^{1,2} · Mengting Li^{1,2} · Hanyi Fang^{1,2} · Bouhari Altine^{1,2} · Qingyao Liu^{1,2} · Yongxue Zhang^{1,2} · Dexing Zeng³ · Xiaoli Lan^{1,2}

Received: 2 July 2019 / Accepted: 6 November 2019
© Society for Biological Inorganic Chemistry (SBIC) 2019

Abstract

Malignant melanoma is an aggressive cancer with poor prognosis. Very late antigen-4 (VLA-4) is overexpressed in melanoma and many other tumors, making it an attractive target for developing molecular diagnostic and therapeutic agents. We compared Al¹⁸F- and ⁶⁸Ga-labeled LLP2A peptides for PET imaging of VLA-4 expression in melanoma. The peptidomimetic ligand LLP2A was modified with chelator 2-*S*-(4-isothiocyanatobenzyl)-1,4,7-triazacyclononane-1,4,7-triacetic acid (*p*-SCN-Bn-NOTA), and the resulting NOTA-PEG₄-LLP2A peptide was then radiolabeled with Al¹⁸F or ⁶⁸Ga. The two labeled peptides were assayed for in vitro and in vivo VLA-4 targeting efficiency. Good Al¹⁸F and ⁶⁸Ga radiolabeling yields were achieved, and the resulting PET tracers showed good serum stability. In the in vivo evaluation of the B16F10 xenograft mouse model, both tracers exhibited high accumulation with good contrast in static PET images. Compared with ⁶⁸Ga-NOTA-PEG₄-LLP2A, Al¹⁸F-NOTA-PEG₄-LLP2A resulted in relatively higher background, including higher liver uptake (1 h: 20.1 ± 2.6 vs. 15.3 ± 1.7%ID/g, *P* < 0.05; 2 h: 11.0 ± 1.2 vs. 8.0 ± 0.8%ID/g, *P* < 0.05) and lower tumor-to-blood ratios (2.5 ± 0.4 vs. 3.3 ± 0.5 at 1 h, *P* < 0.05; 5.1 ± 0.9 vs. 7.3 ± 0.6 at 2 h, *P* < 0.01) at some time points. The results obtained from the mice blocked with unlabeled peptides and VLA-4-negative A375 xenografts groups confirmed the high specificity of the developed tracers. Despite the relatively high liver uptake, both Al¹⁸F-NOTA-PEG₄-LLP2A and ⁶⁸Ga-NOTA-PEG₄-LLP2A exhibited high VLA-4 targeting efficacy with comparable in vivo performance, rendering them promising candidates for imaging tumors that overexpress VLA-4.

Graphic abstract



Yongkang Gai and Lujie Yuan contributed equally to this work.

Electronic supplementary material The online version of this article (<https://doi.org/10.1007/s00775-019-01742-6>) contains supplementary material, which is available to authorized users.

Extended author information available on the last page of the article

Keywords VLA-4 · Melanoma · Al¹⁸F radiolabeling · ⁶⁸Ga · PET imaging · LLP2A

Introduction

Melanoma is a very aggressive malignant tumor with an increasing incidence, especially among Caucasians, and has become one of the major health problems in Western countries [1]. It is one of the most devastating cancers, and is resistant to most treatments. Despite recent advances in the treatment of malignant melanomas, the overall 5-year-survival rate is < 10% [2]. Early diagnosis and accurate staging are important for the choice of appropriate therapeutic interventions to improve patient outcomes.

Noninvasive imaging techniques, including ¹⁸F-fluorodeoxyglucose-based positron emission tomography/computed tomography (PET/CT), play an increasingly critical role in the staging of melanoma and for assessing the response to treatment [3–5]. However, limitations of ¹⁸F-FDG-PET have been described in detecting distant small metastatic lesions, such as sentinel lymph node deposits in stages I and II of this cancer [6, 7]. In addition, the high accumulation of ¹⁸F-FDG in infectious and inflammatory lesions may mimic tumor deposits [8]. With the rapid growth of molecular imaging and precision medicine in the last decades, many radiopharmaceuticals that bind receptors have been developed for more specific imaging of melanoma [9]. Some, including radiolabeled benzamides that target melanin [10–13], α -melanocyte-stimulating hormone analogues that bind to the melanocortin-1 receptor (MC1R) [14–16], and peptides that bind to the integrin family [17–19], have exhibited promising results.

Very late antigen-4 (VLA-4, also called integrin $\alpha_4\beta_1$) is a non-covalent, heterodimeric transmembrane receptor. It is overexpressed in melanoma, and plays a vital role in tumor progression, angiogenesis and metastasis by promoting adhesion and migration of tumor cells [20–22]. Enhanced VLA-4 expression has also been found in lymphomas, leukemias, osteosarcoma, and multiple myeloma [23]. Peptidomimetic LLP2A is a recently discovered VLA-4 targeting ligand with a very high affinity ($IC_{50} = 2$ pM) [24]. Many radionuclides, including ⁶⁴Cu [25–27], ⁶⁸Ga [27, 28], ¹⁸F [29, 30], ¹¹¹In [31], ^{99m}Tc [32], and ¹⁷⁷Lu [33] have been successfully attached to this ligand for diagnosis and/or therapy of VLA-4-abundant tumors. Good images with high tumor-to-background contrasts have been obtained in different animal models [25–33]. In a mouse melanoma model, the ¹⁷⁷Lu-LLP2A bioconjugate showed promising therapeutic efficacy, especially when combined with immune checkpoint inhibitor therapy [34]. It also has shown great therapeutic potential in the treatment of melanoma metastases [33]. There has been clinical success with theranostic combinations of ⁶⁸Ga- and ¹⁷⁷Lu-labeled somatostatin ligands

and prostate-specific membrane antigen (PSMA)-targeted ligands [35–39]. LLP2A-based diagnostic and therapeutic agents have also shown great potential in the treatment of VLA-4-overexpressing melanomas.

¹⁸F is the most commonly used radionuclide for PET with a favorable half-life (109.78 min), high imaging resolution, and good scalability to GBq levels via on-demand cyclotron production. It can be labeled to ligands via the attached 1,4,7-triazacyclononane-1,4,7-triacetic acid (NOTA) chelator by Al¹⁸F chelating. In addition to ¹⁸F, ⁶⁸Gallium (half-life = 67.71 min) has been increasingly considered as a promising radionuclide for routine clinical PET imaging. It is conveniently produced from an in-house ⁶⁸Ge/⁶⁸Ga generator, and has a very simple radiolabeling procedure. Both ¹⁸F and ⁶⁸Ga have their own intrinsic advantages and attract most of the interest in constructing peptide-based tracers. Few attempts have been made to develop ⁶⁸Ga- and ¹⁸F-BF₃-labeled LLP2A peptide for melanoma imaging [27–30], and there has been no direct comparison between ⁶⁸Ga- and ¹⁸F-labeled LLP2A. We prepared a new Al¹⁸F-labeled LLP2A using a one-step Al¹⁸F-chelation method, and assessed its performance in B16F10 (VLA-4-positive) and A375 (VLA-4-negative) mouse models. The results were compared with those obtained from ⁶⁸Ga-NOTA-PEG₄-LLP2A. Characterization and biological evaluations of the labeled peptides included LogP values, serum stability, cell uptake, cell internalization, PET imaging, and ex vivo biodistribution.

Materials and methods

Reagents and instruments

All chemicals were obtained from J&K Chemicals (Beijing, China), or Sigma-Aldrich (St. Louis, MO, USA) and were used without further purification. The mass spectrometry spectra were recorded on Bruker SolarX 7.0T (Germany). Radioactivity was quantified using a dose calibrator (CRC-15R, Capintec, Ramsey, NJ, USA) or gamma counter (2470 WIZARD; PerkinElmer, Waltham, MA, USA). For purification of peptides and analysis of the radiolabeled conjugates using two elution buffers [0.1 v% trifluoroacetic acid (TFA) in deionized water as elution buffer A and 0.1 v% TFA in acetonitrile as elution buffer B], high-performance liquid chromatography (HPLC) was performed on an LC-20AT system (Shimadzu Corporation, Tokyo, Japan) equipped with an SPD-20A UV/vis detector (Shimadzu) and a flow count radiation detector (Bioscan, Washington, DC, USA).

Peptide synthesis

LLP2A was prepared via standard 9-fluorenylmethoxycarbonyl (Fmoc)-based solid phase synthesis as reported previously [24]. Briefly, Fmoc-Lys(Dde)-OH was first attached to Rink amide resin followed by Fmoc-PEG₄-CH₂COOH, Fmoc-Ach-OH, Fmoc-Aad(tBu)-OH, *N*- α -Fmoc-Lys(Alloc)-OH, 2-(4-(3-*o*-tolylureido)phenyl)acetic acid, and Trans-3-(3-pyridyl)acrylic acid. All coupling was performed in dimethylformamide (DMF) using *O*-(7-azabenzotriazol-1-yl)-*N,N,N',N'*-tetramethyluronium hexafluorophosphate (HATU) (3 equivalents), 1-hydroxybenzotriazole (HOBt) (3 equivalents), and *N,N*-diisopropylethylamine (DIEA, 9 equivalents) as coupling reagents. After all the coupling, the Dde protecting group was cleaved with 2% hydrazine in DMF (3 \times 20 min), washed with DMF and dichloromethane (DCM), and cleaved from the resin by twice treating with TFA/Phenol/H₂O/triisopropylsilane (92.5/2.5/2.5/2.5) for 2 h at room temperature. The solution was filtered and the peptide was precipitated in cold diethyl ester. The crude peptide was purified on a semi-preparative C18 column (Sepax GP-C18, 250 \times 10 mm) using HPLC. Fractions from 12.5 to 15 min were collected and lyophilized to obtain pure PEG₄-LLP2A. HPLC method: 0–3 min, 25% buffer B; 3–30 min, from 25% buffer B to 40% buffer B; flow rate, 4 mL/min.

Synthesis of NOTA-PEG₄-LLP2A

p-SCN-Bn-NOTA (1.9 mg) and DIEA (10 μ L) were added to a solution of LLP2A-PEG₄ (2.0 mg) in DMF (0.2 mL). After reaction at room temperature for 4 h, 0.8 mL water was added, and followed by HPLC purification. 2.1 mg product was obtained after lyophilization (yield, ~71%). HPLC method: Sepax GP-C18 (250 \times 4.6 mm), 0–3 min, from 10% buffer B to 20% buffer B; 3–23 min, from 20% buffer B to 60% buffer B; flow rate 1 mL/min. Retention time: 16.1 min. HRMS (Bruker Solarix 7.0T): calcd. for C₇₉H₁₁₁N₁₅O₂₀S: *m/z* [M + 2H]²⁺ 811.9003; observed, [M + H]²⁺ = 811.9000.

Synthesis of nonradioactive Ga- and AIF-NOTA-PEG₄-LLP2A

For Ga-NOTA-PEG₄-LLP2A: NOTA-PEG₄-LLP2A (20 μ L, 5 mM) and GaCl₃ (2 μ L, 100 mM) were added to sodium acetate buffer (50 μ L, 0.25 M, pH 4.5). The mixture was heated at 100 °C for 10 min and the pH was monitored and kept at 4–5. Then, HPLC purification was performed and the peak at 16.0 min was collected. HRMS (Bruker Solarix 7.0T): calcd. for C₇₉H₁₀₈GaN₁₅O₂₀S: *m/z* [M + 2H]²⁺

844.8514; observed, [M + H]²⁺ = 844.8493. The same HPLC method as NOTA-PEG₄-LLP2A was used for this chemical.

For AIF-NOTA-PEG₄-LLP2A: AlCl₃ (100 μ L, 200 mM) and NaF (100 μ L, 200 mM) were mixed and shook for 10 min at room temperature to obtain AIF²⁺ solution. NOTA-PEG₄-LLP2A (20 μ L, 5 mM) and AIF²⁺ solution (2 μ L, 100 mM) were added to sodium acetate buffer (50 μ L, 0.25 M, pH 4.5). The mixture was heated at 100 °C for 10 min and the pH was monitored and kept at 4–5. Then, HPLC purification was performed and the peak at 15.9 min was collected. HRMS (Bruker Solarix 7.0T): calcd. for C₇₉H₁₀₈AlFN₁₅O₂₀S: *m/z* [M + 2H]²⁺ 833.3786; observed, [M + H]²⁺ = 833.3889. The same HPLC method as NOTA-PEG₄-LLP2A was used for this chemical.

Radiolabeling

Al¹⁸F labeling: no-carrier-added ¹⁸F-fluoride was used, which was produced by a GE MINITRACE cyclotron via the ¹⁸O(p,n)¹⁸F reaction. Briefly, the target was washed with 4 mL water to collect residual activity after routine clinical ¹⁸F-FDG production. The target water was passed through a Sep-Pak QMA light cartridge (Waters), which was pre-conditioned with 5 mL of 0.5 M potassium bicarbonate. The ¹⁸F was eluted with 300 μ L saline and the fractions were collected into six tubes (each 50 μ L). To the tube containing the highest activity (500–740 MBq), AlCl₃ (2 μ L, 5 mM in sodium acetate buffer, pH 4, 0.1 M), sodium acetate buffer (10 μ L, pH 4, 1 M), acetonitrile (50 μ L) and NOTA-PEG₄-LLP2A (4 μ L, 5 mM) were added. The solution was heated at 100 °C for 15 min, and then diluted with 1 mL water. The resulting mixture passed through a C18 light cartridge (Waters), followed by washing the cartridge with 5 mL water to remove unreacted ¹⁸F, and then the desired Al¹⁸F-NOTA-PEG₄-LLP2A was eluted with 0.5 mL ethanol. The product was reconstituted in saline and passed through a 0.22 μ m Millipore filter into a sterile vial, and its radiochemical purity was determined by radio-HPLC.

⁶⁸Ga labeling: ⁶⁸Ga³⁺ in 0.05 M HCl was obtained from a ⁶⁸Ge/⁶⁸Ga generator (Isotope Technologies Graching, Germany). Briefly, 4 mL 0.05 M HCl was passed through the column and the fractions were collected into eight tubes (each 0.5 mL). Sodium acetate buffer (150 μ L, 0.25 M, pH 4.5) and NOTA-PEG₄-LLP2A (2 μ L, 5 mM) were added to the tube containing the highest activity (370–500 MBq). The pH of the final radiolabeling solution was 4–5. Then, the mixture was heated at 100 °C for 10 min. The radiolabeling yield of the product ⁶⁸Ga-NOTA-PEG₄-LLP2A was determined by radio-HPLC.

Radio-HPLC method: 0–4 min, 5% buffer B; 4–5 min, from 5% buffer B to 90% buffer B; 5–10 min, 90% buffer B; 10–15 min, 5% buffer B; flow rate, 1.0 mL/min.

Serum stability

Al¹⁸F-NOTA-PEG₄-LLP2A and ⁶⁸Ga-NOTA-PEG₄-LLP2A (~3.7 MBq) were each mixed with 0.5 mL human serum, and the two mixtures were incubated at 37 °C for 4 h (Al¹⁸F-tracer) and 2 h (⁶⁸Ga-tracer), respectively. To remove plasma protein, 0.5 mL acetonitrile was added to the mixtures, followed by 5 min centrifugation at 14,000 rpm. The supernatants were separated and 90% of the radioactivity was recovered. Approximately 37 kBq of the supernatants was taken for radioactive purity determination using radio-HPLC. Free ⁶⁴Cu/⁶⁸Ga came out at ~3.5 min and the radiolabeled conjugates came out at 11 min.

Cell culture

Cells were cultured in Dulbecco's Modified Eagle Medium (DMEM), supplemented with 10% fetal bovine serum, penicillin (100 units/mL), streptomycin (100 µg/mL) L-glutamine (300 µg/mL), sodium pyruvate (100 mg/mL), and glucose (4.5 g/L) and maintained at 37 °C, 5% CO₂.

Cell uptake and internalization

B16F10 cells were seeded in 12-well plates (200,000 cells per well) 24 h prior to the experiment. The cells were then washed twice with 1 mL Hank's Balanced Salt Solution (HBSS) and 1 mL media (DMEM with 0.1% BSA and 1 mM Mn²⁺) was added to each well. The cells were then incubated with Al¹⁸F-NOTA-PEG₄-LLP2A/⁶⁸Ga-NOTA-PEG₄-LLP2A (~74 kBq per well) with and without the addition of excess LLP2A-PEG₄ (10 µg per well) to determine nonspecific uptake. At different time points (0.5, 1, and 2 h for ⁶⁸Ga-tracer; 0.5, 1, 2, and 4 h for ¹⁸F-tracer), the radioactive media were aspirated, and the plate was washed twice with PBS buffer (pH 7.2). The total cell uptakes were measured by counting the radioactivity on a gamma counter. To collect the surface-bound fraction, each well was treated with 20 mM sodium acetate-HBSS (pH 4.0) and was incubated at 37 °C for 10 min. After removal of the surface-bound fraction, cell pellets were dissolved in 0.5% SDS. All of the fractions were counted in a well counter (2470 Automatic Gamma Counter WIZARD, PerkinElmer, Norwalk, CT, USA). The amount internalized was the amount of activity in the final cell pellet, corrected for activity in the blocked fractions and background activity. The percentages of the radiotracers internalized into the cell were calculated based on the equation: (the gamma counts obtained from cell-internalized radioactivity)/(the gamma counts obtained from the total cell-associated radioactivity).

Animal model

Four-week-old female C57BL/6 and BALB/c nude mice purchased from HFK Bioscience (Beijing, China) were used in this study. All mice were maintained under specific pathogen-free conditions, within facilities approved by the Laboratory Animal Care of Huazhong University of Science and Technology, and in compliance with the regulations and standards of the Institutional Animal Care and Use Committee of Tongji Medical College of Huazhong University of Science and Technology. For B16F10 and A375 tumor xenografts, C57BL/6 and BALB/c nude mice were injected subcutaneously in the right shoulder with one million cells in PBS buffer, respectively.

Micro-PET imaging

Mice bearing B16F10/A375 xenografts (4 mice per group) were injected intravenously with Al¹⁸F-NOTA-PEG₄-LLP2A or ⁶⁸Ga-NOTA-PEG₄-LLP2A (5.5–7.4 MBq, 100–200 pmol per mouse) with or without a blocking dose (100 µg unlabeled LLP2A-PEG₄). At 0.5 h, 1 h and 2 h (and 4 h for ¹⁸F) post injection (p.i.), mice were anesthetized with 2% isoflurane and PET images were acquired. All PET scans were performed with a small-animal PET scanner (BioCalibur LH Raycan Technology Co., Ltd.TM, Suzhou, China). The intrinsic spatial resolution was 1.0 mm, the time resolution was 1.50 ns full-width at half-maximum, the energy resolution was 13.0% at 511 keV and the axial field of view was 5.3 cm.

Ex vivo biodistribution

Mice bearing B16F10/A375 xenografts (5 mice per group) were injected intravenously with Al¹⁸F-NOTA-PEG₄-LLP2A or ⁶⁸Ga-NOTA-PEG₄-LLP2A (5.5–7.4 MBq, 100–200 pmol per mouse) with or without a blocking dose (100 µg unlabeled LLP2A-PEG₄). The tumor-bearing mice were killed at 0.5 h, 1 h, and 2 h (and 4 h for ¹⁸F-tracer) p.i.. The organs and tumors were harvested, weighed, and counted in a gamma counter. The radioactivity in each tissue was normalized as the percentage injected dose per gram of tissue (%ID/g).

Statistics analysis

Significance analysis of the data was performed by unpaired *t*-testing using Prism software (GraphPad Software Inc., San Diego, CA, USA). Multiple comparisons were performed by multiple *t*-tests together with the Holm–Sidak method for correction. A value of *P* < 0.05 was considered significant and *P* < 0.01 was considered highly significant.

Results

Synthesis and radiolabeling

A good isolated yield (~50%) of $\text{NH}_2\text{-PEG}_4\text{-LLP2A}$ was obtained from the traditional Fmoc-based solid phase synthesis. *p*-SCN-Bn-NOTA was attached to the prepared $\text{NH}_2\text{-PEG}_4\text{-LLP2A}$ with a 71% yield; after HPLC purification, the purity of the $\text{NOTA-PEG}_4\text{-LLP2A}$ product was >95% (see Fig. 1a for the structures).

The Al^{18}F radiolabeling of the conjugate was performed at 100 °C in 0.1 M sodium acetate buffer (pH 4) for 15 min. Radiochemical yields ranging from 38 to 42% were obtained with high radiochemical purity (>95%). The ^{68}Ga radiolabeling of the conjugate was performed at 100 °C in a solution of 0.5 mL $^{68}\text{GaCl}_3$ in HCl (0.05 M) and 0.15 mL sodium acetate (0.25 M) for 15 min. A greater than 95% radiolabeling yield was achieved. Nonradioactive $\text{Ga-NOTA-PEG}_4\text{-LLP2A}$ and $\text{AlF-NOTA-PEG}_4\text{-LLP2A}$ standards were prepared to confirm the successful ^{68}Ga and Al^{18}F radiolabeling. The molar activity of $^{68}\text{Ga-NOTA-PEG}_4\text{-LLP2A}$ (37–74 MBq/nmol) was slightly higher than that of $\text{Al}^{18}\text{F-NOTA-PEG}_4\text{-LLP2A}$ (20–37 MBq/nmol). Both $\text{Al}^{18}\text{F}^{2+}$ and $^{68}\text{Ga}^{3+}$ labeled tracers exhibited good stability, and less than 5% disassociation of ^{18}F and ^{68}Ga were observed after being incubated in human serum at 37 °C (Fig. 1b). The $\text{Log}P$ values of

$\text{Al}^{18}\text{F-NOTA-PEG}_4\text{-LLP2A}/^{68}\text{Ga-NOTA-PEG}_4\text{-LLP2A}$ were -1.80 ± 0.03 and -1.92 ± 0.05 , respectively, indicating that both tracers were hydrophilic.

In vitro cell study

To determine the specific binding and internalization profiles of $\text{Al}^{18}\text{F-NOTA-PEG}_4\text{-LLP2A}$ and $^{68}\text{Ga-NOTA-PEG}_4\text{-LLP2A}$, cell uptake studies were performed using the VLA-4 overexpressing mouse B16F10 melanoma cells. 4 h and 2 h cell uptake studies were conducted for ^{18}F - and ^{68}Ga -tracers, respectively, because of their different half-life times. As shown in Fig. 1c, e, the uptake of $\text{Al}^{18}\text{F-NOTA-PEG}_4\text{-LLP2A}$ increased within 1 h and then remained at a plateau up to 4 h, while the uptake of $^{68}\text{Ga-NOTA-PEG}_4\text{-LLP2A}$ gradually increased over 2 h. The uptake values of $^{68}\text{Ga-NOTA-PEG}_4\text{-LLP2A}$ were significantly higher than those of $\text{Al}^{18}\text{F-NOTA-PEG}_4\text{-LLP2A}$ at the same time point ($P < 0.01$). A total of 32.0–35.5% (Al^{18}F -tracer) and 26.9–36.5% (^{68}Ga -tracer) of the cell-bonded tracers (1–1.4% and 2.2–2.4% of total added dose, respectively) were internalized into the cells, while most of them remained on the cell surface. In the groups receiving the blocking dose, the uptake of $\text{Al}^{18}\text{F-NOTA-PEG}_4\text{-LLP2A}$ and $^{68}\text{Ga-NOTA-PEG}_4\text{-LLP2A}$ were reduced significantly by 61.7 and 79.2%, respectively, validating their high specificity for VLA-4.

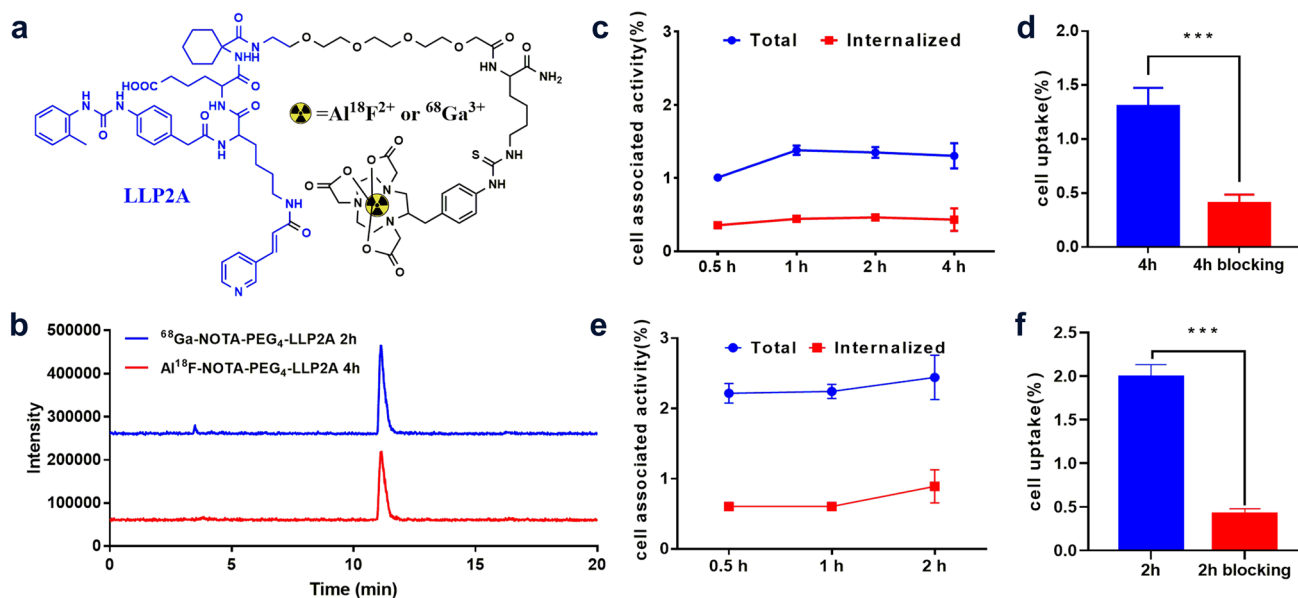
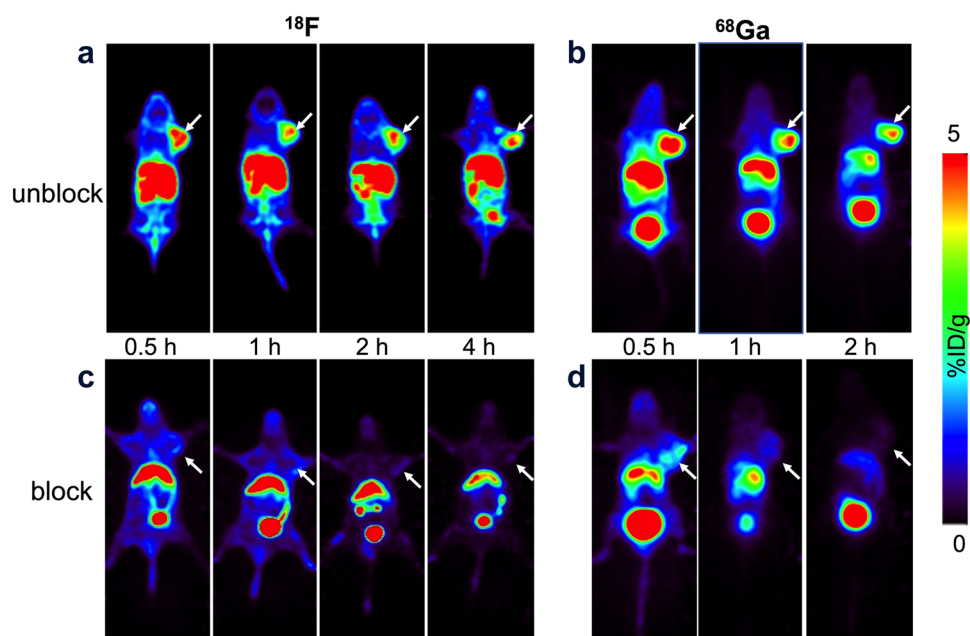


Fig. 1 a Structures of $\text{Al}^{18}\text{F-NOTA-PEG}_4\text{-LLP2A}$ and $^{68}\text{Ga-NOTA-PEG}_4\text{-LLP2A}$. b Stability of $\text{Al}^{18}\text{F-NOTA-PEG}_4\text{-LLP2A}$ and $^{68}\text{Ga-NOTA-PEG}_4\text{-LLP2A}$ after incubation in serum at 37 °C for 4 h and 2 h, respectively. c, e Cell internalization of $\text{Al}^{18}\text{F-NOTA-PEG}_4\text{-LLP2A}$ and $^{68}\text{Ga-NOTA-PEG}_4\text{-LLP2A}$ in B16F10 cells. The radioactivity that was removed from the cells by treatment with 20 mM sodium acetate-HBSS (pH 4.0) was consid-

ered as the membrane-bound fraction. The radioactivity measured in the cell lysates was considered as the internalized fraction. Total cell-associated activity equals the activity of internalized fraction plus membrane-bound fraction. d, f B16F10 cell uptake of the two tracers and after blocking with co-incubation of 10 μg unlabeled LLP2A-PEG_4 (***) ($P < 0.001$; $n = 3$)

Fig. 2 Representative static PET images of the B16F10 xenograft at 0.5 h, 1 h, 2 h, and 4 h p.i. of 5.5–7.4 MBq (100–200 pmol) Al^{18}F -NOTA-PEG₄-LLP2A (**a**) and ^{68}Ga -NOTA-PEG₄-LLP2A (**b**), and the blocked group co-injected with 100 μg unlabeled LLP2A-PEG₄ (**c** and **d**, respectively). Arrows indicate tumors



Small-animal PET imaging

The static images of Al^{18}F -NOTA-PEG₄-LLP2A in mice bearing B16F10 tumors afforded excellent tumor visualization with high tumor retention and tumor-to-background contrast at 0.5 h, 1 h, 2 h and 4 h after intravenous injection. The activity accumulation in liver was high and minimal activity accumulations were observed in other normal organs, except bladder.

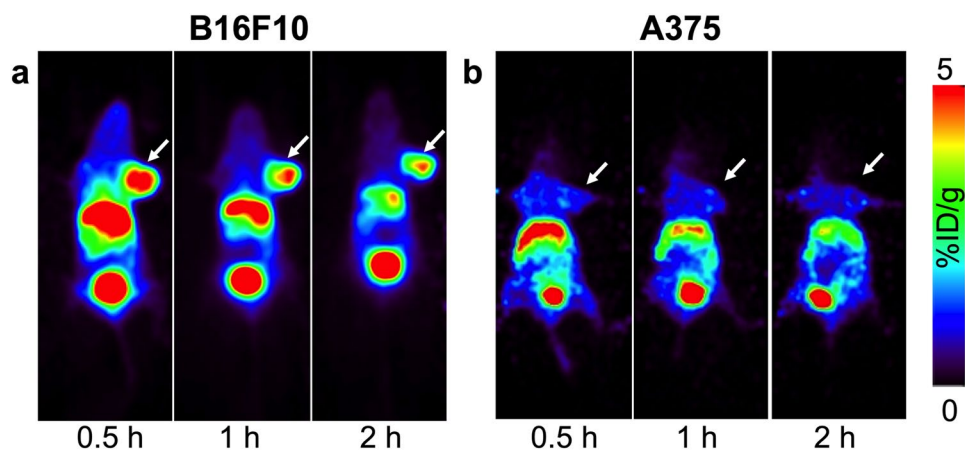
PET images obtained from the group injected with ^{68}Ga -NOTA-PEG₄-LLP2A tracers were similar to those injected with Al^{18}F -NOTA-PEG₄-LLP2A, and all the tumors were clearly visualized with highest tumor uptake achieved at an early p.i. time point (0.5 h). Compared to Al^{18}F -NOTA-PEG₄-LLP2A, ^{68}Ga -NOTA-PEG₄-LLP2A showed faster clearance and also slightly less liver uptake, with higher bladder uptake due to the renal excretion of injected radioactivity.

To validate *in vivo* specificity, blocking doses were applied to the mice injected with Al^{18}F -NOTA-PEG₄-LLP2A and ^{68}Ga -NOTA-PEG₄-LLP2A. As shown in Fig. 2c, d, the activity accumulation in B16F10 xenografts was significantly reduced by the blocking agent, showing good specificity. To further confirm their VLA-4 targeting specificity, mice bearing VLA-4-negative A375 xenografts were injected with ^{68}Ga -NOTA-PEG₄-LLP2A and PET imaging was conducted at the same time points. The resulting PET images did not show specific accumulation in the A375 xenografts (Fig. 3).

Ex vivo biodistribution

Biodistribution data are summarized in Figs. 4 and 5 and Tables S1, S2 (see electronic supplementary material). Both Al^{18}F -NOTA-PEG₄-LLP2A and ^{68}Ga -NOTA-PEG₄-LLP2A exhibited similar *in vivo* distribution and excretion

Fig. 3 Representative static PET images of C57BL/6 mice bearing B16F10 tumor xenografts (**a**) and BALB/c nude mice bearing A375 tumor xenografts (**b**) at 0.5 h, 1 h, and 2 h p.i. of 5.5–7.4 MBq (100–200 pmol) ^{68}Ga -NOTA-PEG₄-LLP2A. Arrows indicate tumors



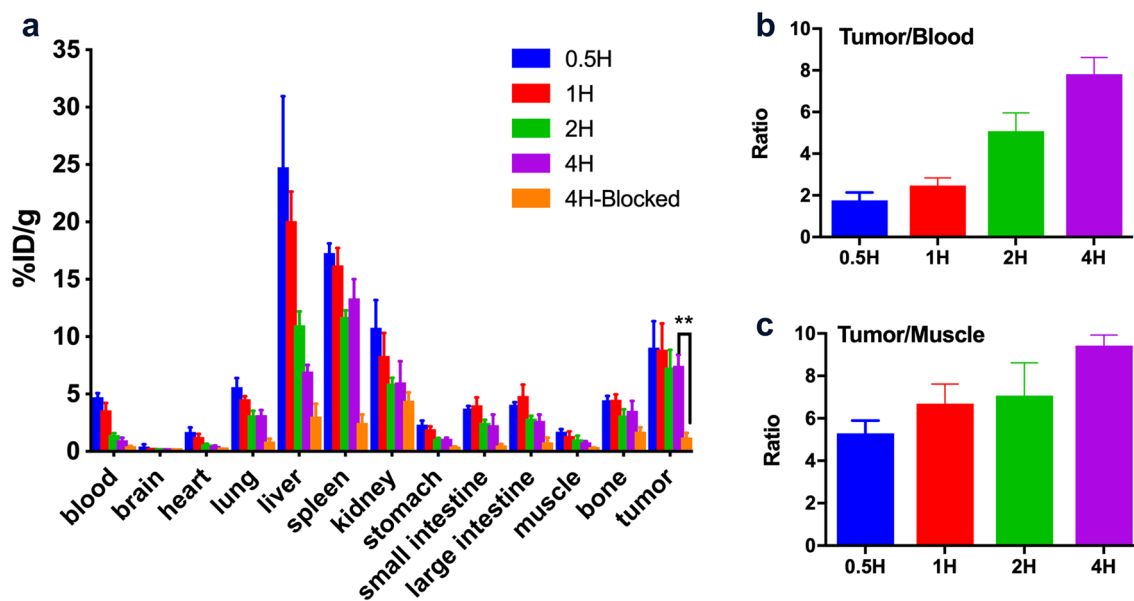


Fig. 4 Biodistribution in mice bearing B16F10 tumors at 0.5 h, 1 h, 2 h and 4 h p.i. of $Al^{18}F$ -NOTA-PEG₄-LLP2A (5.5–7.4 MBq, 100–200 pmol) and 4 h after blocking by coinjection of 100 μ g unlabeled

LLP2A-PEG₄ with the $Al^{18}F$ -NOTA-PEG₄-LLP2A) (a); tumor-to-blood ratios (b); tumor-to-muscle ratios (c) ($n=5$, $**P<0.001$)

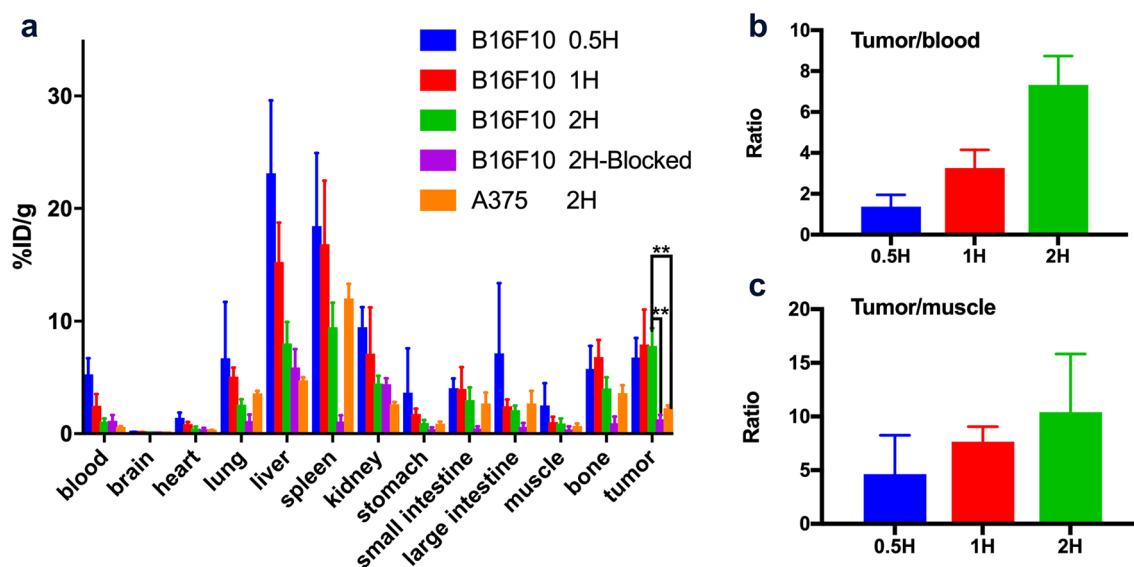


Fig. 5 Biodistribution of ^{68}Ga -NOTA-PEG₄-LLP2A (5.5–7.4 MBq, 100–200 pmol) in mice bearing B16F10 tumors at 0.5 h, 1 h and 2 h p.i., 2 h blocked (co-injected with 100 μ g unlabeled LLP2A-PEG₄ with the ^{68}Ga -NOTA-PEG₄-LLP2A), and in mice bearing A375

tumors at 2 h p.i. (a); tumor-to-blood ratios (b) and tumor-to-muscle ratios (c) of ^{68}Ga -NOTA-PEG₄-LLP2A in mice bearing B16F10 tumors at 0.5, 1 and 2 h post-injection ($n=5$, $**P<0.001$)

profiles, such as high uptake in tumor, liver, spleen, and kidneys at the same time point p.i.. Both tracers cleared from the kidneys and liver; however, the liver clearance was significantly higher for $Al^{18}F$ -NOTA-PEG₄-LLP2A than for ^{68}Ga -NOTA-PEG₄-LLP2A at 1 h and 2 h p.i. (1 h: 20.1 ± 2.6 vs. 15.3 ± 1.7 %ID/g, $P < 0.05$; 2 h: 11.0 ± 1.2

vs. 8.0 ± 0.8 %ID/g, $P < 0.05$). Significantly lower uptake in the colon was observed for ^{68}Ga -NOTA-PEG₄-LLP2A than for $Al^{18}F$ -NOTA-PEG₄-LLP2A at 1 h and 2 h p.i. (1 h: 4.8 ± 0.9 vs. 2.4 ± 0.3 %ID/g, $P < 0.01$; 2 h: 2.8 ± 0.2 vs. 2.1 ± 0.2 %ID/g, $P < 0.01$). The kidney uptake was also significantly lower for ^{68}Ga -NOTA-PEG₄-LLP2A than

for Al¹⁸F-NOTA-PEG₄-LLP2A at 2 h p.i. (5.9 ± 0.5 vs. $4.5 \pm 0.3\%$ ID/g, $P < 0.01$). The biodistribution comparisons of Al¹⁸F-NOTA-PEG₄-LLP2A and ⁶⁸Ga-NOTA-PEG₄-LLP2A are shown in Figure S1.

Discussion

The aim of this study was to develop LLP2A-based PET tracers using same peptidomimetic precursor, with different positron emitters (¹⁸F and ⁶⁸Ga), and compare their in vivo performance for PET imaging of melanoma. A commonly used chelator, *p*-SCN-Bn-NOTA, served as the key coordinating group to form stable complexes with Al¹⁸F and ⁶⁸Ga. To our knowledge, this is the first report of an Al¹⁸F-labeled LLP2A tracer. Previously, there have been only a few reports of ¹⁸F-labeled LLP2A using the ¹⁸F-organotrifluoroborate method [29, 30]. In their study, PEG₂-LLP2A-trifluoroborate conjugates were synthesized and labeled with ¹⁸F by the isotope exchange method with sufficient molar activity but relatively lower radiochemical yields of 3.7% and 11.3%, respectively.

Stability is extremely important for radiotracers, especially for ¹⁸F radiolabeled tracers, since free ¹⁸F⁻ binds to bone with high affinity. Thus, we conducted an in vitro stability test, and both prepared tracers remained intact after several hours' incubation in serum and PBS. For Al¹⁸F-NOTA-PEG₄-LLP2A, relatively high bone uptake ($4.47 \pm 0.37\%$ ID/g at 0.5 h) was determined by an ex vivo biodistribution study. The high bone uptake usually indicates defluorination and low in vivo stability of ¹⁸F-based tracers. In this case, defluorination might also occur for Al¹⁸F-NOTA-PEG₄-LLP2A, however, the majority was most likely contributed by marrow uptake because of the natural expression of VLA-4 in the bone marrow [40]. Moreover, higher bone uptake ($5.75 \pm 2.04\%$ ID/g at 0.5 h) was also observed in mice receiving ⁶⁸Ga-NOTA-PEG₄-LLP2A, which confirmed specific uptake in bone marrow. The bone uptake was significantly reduced for both tracers when cold PEG₄-LLP2A was co-injected, which further validated the stability.

All tumors could be clearly visualized in the PET images with high retention up to 4 h and 2 h p.i. of ¹⁸F- or ⁶⁸Ga-labeled tracers, respectively. The tumor uptake values of the two tracers were comparable at the same time points p.i. post injection, except a slightly higher tumor uptake of Al¹⁸F-NOTA-PEG₄-LLP2A ($9.04 \pm 2.30\%$ ID/g) at 0.5 h than ⁶⁸Ga-NOTA-PEG₄-LLP2A ($6.77 \pm 1.77\%$ ID/g) without statistical significance. ⁶⁸Ga-NOTA-PEG₄-LLP2A had significantly higher tumor-to-blood ratios at 1 h ($P < 0.05$) and 2 h ($P < 0.01$), and significantly higher tumor-to-muscle ratio at 2 h ($P < 0.05$) than Al¹⁸F-NOTA-PEG₄-LLP2A. It should be noticed that the molar activity of ⁶⁸Ga-NOTA-PEG₄-LLP2A

(37–74 MBq/nmol) was slightly higher than that of Al¹⁸F-NOTA-PEG₄-LLP2A (20–37 MBq/nmol), which might also contribute to the superior in vivo performance of ⁶⁸Ga-NOTA-PEG₄-LLP2A. The tumor uptake of ⁶⁸Ga-NOTA-PEG₄-LLP2A at 1 h was comparable to that of ⁶⁸Ga-DOTA-PEG₄-LLP2A [33] ($9.1 \pm 0.9\%$ ID/g) and ⁶⁸Ga-NODAGA-PEG₄-LLP2A [27] ($8.7 \pm 1.3\%$ ID/g) without statistical significance. The tumor uptake of Al¹⁸F-NOTA-PEG₄-LLP2A at 1 h was comparable to that of ¹⁸F-DOTA-AMBF₃-PEG₂-LLP2A ($9.46 \pm 2.19\%$ ID/g) [30], but significantly higher than that of ¹⁸F-N-Pyr-*p*-BF₃⁻-PEG₂-LLP2A ($4.41 \pm 0.65\%$ ID/g, $P = 0.001$) and ¹⁸F-AMBF₃-PEG₂-LLP2A ($2.84 \pm 0.34\%$ ID/g, $P < 0.0001$) [29]. ⁶⁸Ga-NOTA-PEG₄-LLP2A exhibited relatively quicker clearance from nonspecific organs, which might be due to slightly lower lipophilicity than Al¹⁸F-NOTA-PEG₄-LLP2A. It is consistent with their Log*P* profiles. The specificity of Al¹⁸F-NOTA-PEG₄-LLP2A and ⁶⁸Ga-NOTA-PEG₄-LLP2A was validated via blocking study, and further confirmed using a VLA-4-negative A375 tumor model.

Liver and bladder showed the most intense uptake, and the activity accumulation in liver decreased over time, indicating both tracers cleared predominantly via the hepatobiliary pathway and partly via renal clearance. Significantly higher liver uptake was observed at 1 h and 2 h p.i. of Al¹⁸F-NOTA-PEG₄-LLP2A compared to those of ⁶⁸Ga-NOTA-PEG₄-LLP2A ($P < 0.01$). The overall liver uptake of Al¹⁸F-NOTA-PEG₄-LLP2A and ⁶⁸Ga-NOTA-PEG₄-LLP2A was significantly higher than those of ⁶⁸Ga-NODAGA-PEG₄-LLP2A [27] and our previously reported ⁶⁸Ga-NE2P1A-PEG₄-LLP2A [28], which might be due to the slightly higher lipophilicity of the chelator *p*-SCN-Bn-NOTA than those of NODAGA and *p*-SCN-PhPr-NE2P1A. Compared to the reported ¹⁸F-R-BF₃-PEG₂-LLP2A tracers, the liver uptake of Al¹⁸F-NOTA-PEG₄-LLP2A was relatively higher, but the colon uptake was much lower [29]. The high colonic uptake of ¹⁸F-R-BF₃-PEG₂-LLP2A was significantly reduced by introducing an appended DOTA moiety, which usually serves as a metal chelator, but acted as a hydrophilic appendant in their study [30]. The relatively high liver uptake of Al¹⁸F-NOTA-PEG₄-LLP2A and ⁶⁸Ga-NOTA-PEG₄-LLP2A may hinder their applications in the detection of liver metastatic lesions, which might also be solved by introducing a hydrophilic appendant.

Overall, ⁶⁸Ga-NOTA-PEG₄-LLP2A displayed clear superiority, compared with Al¹⁸F-NOTA-PEG₄-LLP2A, due to significantly lower liver uptake, and significantly higher tumor-to-muscle and tumor-to-blood ratios at some time points. Considering the wide availability of ¹⁸F⁻, development of ¹⁸F-labeled VLA-4 tracers may also be in demand in situations where the supply of ⁶⁸Ga (and/or ⁶⁸Ge/⁶⁸Ga generators) is limited. In addition, the residual activity of ¹⁸F after routine ¹⁸F-FDG production was collected by

washing the target of the cyclotron and used for the production of Al¹⁸F-NOTA-PEG₄-LLP2A in this study. Much larger amounts of Al¹⁸F-NOTA-PEG₄-LLP2A can be produced with higher specific activity when the entire activity produced by the cyclotron is used. Thus, Al¹⁸F-NOTA-PEG₄-LLP2A is a good alternative VLA-4 imaging tracer for research and clinical translation.

Conclusion

In summary, two VLA-4 targeted radiotracers (Al¹⁸F-NOTA-PEG₄-LLP2A and ⁶⁸Ga-NOTA-PEG₄-LLP2A) have been successfully constructed for PET imaging of melanoma, and both tracers showed high in vivo VLA-4 targeting efficiency and good specificity. The favorable biodistribution and PET images make them promising candidates for noninvasively imaging VLA-4 overexpressing tumors.

Acknowledgements This work was supported, in part, by the National Natural Science Foundation of China (Nos. 81801738 and 81630049), the Fundamental Research Fund for the Chinese Central Universities of Huazhong University of Science and Technology (2017KIFYXJJ235), opening foundation of Hubei key laboratory of molecular imaging (02.03.2017-187) and research foundation of Wuhan Union Hospital (02.03.2017-12). We also acknowledge the support from the National Institute of Biomedical Imaging and Bioengineering grant R21-EB020737, and the American Cancer Society Research Scholar ACS-RSG-17-004-01-CCE.

Compliance with ethical standards

Conflict of interest The authors declare that they have no conflicts of interest.

References

- Welch HG, Woloshin S, Schwartz LM (2005) Skin biopsy rates and incidence of melanoma: population based ecological study. *BMJ* 331(7515):481
- Trinh VA (2008) Current management of metastatic melanoma. *Am J Health Syst Pharm* 65(24 Suppl 9):S3–S9
- Mijnhout GS, Hoekstra OS, van Tulder MW, Teule GJ, Devillé WL (2001) Systematic review of the diagnostic accuracy of 18F-fluorodeoxyglucose positron emission tomography in melanoma patients. *Cancer* 91(8):1530–1542
- Pfannenbergh C, Aschoff P, Schanz S, Eschmann SM, Plathow C, Eigentler TK, Garbe C, Brechtel K, Vonthein R, Bares R (2007) Prospective comparison of ¹⁸F-fluorodeoxyglucose positron emission tomography/computed tomography and whole-body magnetic resonance imaging in staging of advanced malignant melanoma. *Eur J Cancer* 43(3):557–564
- Rinne D, Baum RP, Hör G, Kaufmann R (1998) Primary staging and follow-up of high risk melanoma patients with whole-body ¹⁸F-fluorodeoxyglucose positron emission tomography. *Cancer* 82(9):1664–1671
- Strobel K, Bode B, Dummer R, Veit-Haibach P, Fischer D, Imhof L, Goldinger S, Steinert HC, Von Schulthess G (2009) Limited value of 18 F-FDG PET/CT and S-100B tumour marker in the detection of liver metastases from uveal melanoma compared to liver metastases from cutaneous melanoma. *Eur J Nucl Med Mol Imaging* 36(11):1774
- Servois V, Mariani P, Malhaire C, Petras S, Piperno-Neumann S, Plancher C, Levy-Gabriel C, Lumbroso-le Rouic L, Desjardins L, Salmon R (2010) Preoperative staging of liver metastases from uveal melanoma by magnetic resonance imaging (MRI) and fluorodeoxyglucose-positron emission tomography (FDG-PET). *Eur J Surg Oncol* 36(2):189–194
- Choi EA, Gershenwald JE (2007) Imaging studies in patients with melanoma. *Surg Oncol Clin N Am* 16(2):403–430
- Wei W, Ehlerding EB, Lan X, Luo Q, Cai W (2018) PET and SPECT imaging of melanoma: the state of the art. *Eur J Nucl Med Mol Imaging* 45(1):132–150
- Xu X, Yuan L, Yin L, Jiang Y, Gai Y, Liu Q, Wang Y, Zhang Y, Lan X (2017) Synthesis and preclinical evaluation of ¹⁸F-PEG3-FPN for the detection of metastatic pigmented melanoma. *Mol Pharm* 14(11):3896–3905
- Feng H, Xia X, Li C, Song Y, Qin C, Liu Q, Zhang Y, Lan X (2016) Imaging malignant melanoma with ¹⁸F-5-FPN. *Eur J Nucl Med Mol Imaging* 43(1):113–122
- Ma X, Wang S, Wang S, Liu D, Zhao X, Chen H, Kang F, Yang W, Wang J, Cheng Z (2019) Biodistribution, radiation dosimetry, and clinical application of a melanin-targeted PET probe, ¹⁸F-P3BZA, in patients. *J Nucl Med* 60(1):16–22
- Xu X, Yuan L, Gai Y, Liu Q, Yin L, Jiang Y, Wang Y, Zhang Y, Lan X (2018) Targeted radiotherapy of pigmented melanoma with ¹³¹I-5-IPN. *J Exp Clin Cancer Res* 37(1):306
- Zhang C, Zhang Z, Lin K-S, Pan J, Dude I, Hundal-Jabal N, Colpo N, Bénard F (2017) Preclinical melanoma imaging with ⁶⁸Ga-labeled α -melanocyte-stimulating hormone derivatives using PET. *Theranostics* 7(4):805
- Froidevaux S, Calame-Christe M, Schuhmacher J, Tanner H, Saffrich R, Henze M, Eberle AN (2004) A gallium-labeled DOTA- α -melanocyte-stimulating hormone analog for PET imaging of melanoma metastases. *J Nucl Med* 45(1):116–123
- Zhang C, Zhang Z, Lin K-S, Lau J, Zeisler J, Colpo N, Perrin DM, Bénard F (2018) Melanoma imaging using ¹⁸F-labeled α -melanocyte-stimulating hormone derivatives with positron emission tomography. *Mol Pharm* 15(6):2116–2122
- Pohle K, Notni J, Bussemmer J, Kessler H, Schwaiger M, Beer AJ (2012) ⁶⁸Ga-NODAGA-RGD is a suitable substitute for ¹⁸F-Galacto-RGD and can be produced with high specific activity in a cGMP/GRP compliant automated process. *Nucl Med Biol* 39(6):777–784
- Notni J, Pohle K, Wester H-J (2013) Be spoilt for choice with radiolabelled RGD peptides: preclinical evaluation of ⁶⁸Ga-TRAP (RGD) 3. *Nucl Med Biol* 40(1):33–41
- D'Alessandria C, Pohle K, Rechenmacher F, Neubauer S, Notni J, Wester H-J, Schwaiger M, Kessler H, Beer AJ (2016) In vivo biokinetic and metabolic characterization of the ⁶⁸Ga-labelled α 5 β 1-selective peptidomimetic FR366. *Eur J Nucl Med Mol Imaging* 43(5):953–963
- Holzmann B, Gossler U, Bittner M (1998) α 4 integrins and tumor metastasis. In: *Leukocyte integrins in the immune system and malignant disease*. Springer, Berlin, pp 125–141
- Moretti S, Martini L, Berti E, Pinzi C, Giannotti B (1993) Adhesion molecule profile and malignancy of melanocytic lesions. *Melanoma Res* 3(4):235–239
- Garmy-Susini B, Jin H, Zhu Y, Sung R-J, Hwang R, Varner J (2005) Integrin α 4 β 1-VCAM-1-mediated adhesion between endothelial and mural cells is required for blood vessel maturation. *J Clin Invest* 115(6):1542–1551

23. Schlesinger M, Bendas G (2015) Contribution of very late antigen-4 (VLA-4) integrin to cancer progression and metastasis. *Cancer Metastasis Rev* 34(4):575–591
24. Peng L, Liu R, Marik J, Wang X, Takada Y, Lam KS (2006) Combinatorial chemistry identifies high-affinity peptidomimetics against $\alpha_4\beta_1$ integrin for in vivo tumor imaging. *Nat Chem Biol* 2(7):381
25. Jiang M, Ferdani R, Shokeen M, Anderson CJ (2013) Comparison of two cross-bridged macrocyclic chelators for the evaluation of ^{64}Cu -labeled-LLP2A, a peptidomimetic ligand targeting VLA-4-positive tumors. *Nucl Med Biol* 40(2):245–251
26. Gai Y, Sun L, Hui W, Ouyang Q, Anderson CJ, Xiang G, Ma X, Zeng D (2016) New bifunctional chelator p-SCN-PhPr-NE3TA for copper-64: synthesis, peptidomimetic conjugation, radiolabeling, and evaluation for PET imaging. *Inorg Chem* 55(14):6892–6901
27. Beaino W, Anderson CJ (2014) PET imaging of very late antigen-4 in melanoma: comparison of ^{68}Ga - and ^{64}Cu -labeled NODAGA and CB-TE1A1P-LLP2A conjugates. *J Nucl Med* 55(11):1856–1863
28. Gai Y, Sun L, Lan X, Zeng D, Xiang G, Ma X (2018) Synthesis and evaluation of new bifunctional chelators with phosphonic acid arms for Gallium-68 based PET imaging in melanoma. *Bioconjug Chem* 29(10):3483–3494
29. Roxin A, Zhang C, Huh S, Lepage ML, Zhang Z, Lin K-S, Bénard F, Perrin DM (2018) Preliminary evaluation of ^{18}F -labeled LLP2A-trifluoroborate conjugates as VLA-4 ($\alpha_4\beta_1$ integrin) specific radiotracers for PET imaging of melanoma. *Nucl Med Biol* 61:11–20
30. Roxin A, Zhang C, Huh S, Lepage M, Zhang Z, Lin K, Bénard F, Perrin D (2019) A metal-free DOTA-conjugated ^{18}F -labeled radiotracer: [^{18}F] DOTA-AMBF3-LLP2A for imaging VLA-4 over-expression in murine melanoma with improved tumor uptake and greatly enhanced renal clearance. *Bioconjug Chem*. <https://doi.org/10.1021/acs.bioconjchem.9b00146> (just accepted manuscript)
31. DeNardo SJ, Liu R, Albrecht H, Natarajan A, Sutcliffe JL, Anderson C, Peng L, Ferdani R, Cherry SR, Lam KS (2009) ^{111}In -LLP2A-DOTAPolyethylene glycol-targeting $\alpha_4\beta_1$ integrin: comparative pharmacokinetics for imaging and therapy of lymphoid malignancies. *J Nucl Med* 50(4):625–634
32. Zwingenberger AL, Kent MS, Liu R, Kukis DL, Wisner ER, DeNardo SJ, Taylor SL, Chen X, Lam KS (2012) In-vivo biodistribution and safety of $^{99\text{m}}\text{Tc}$ -LLP2A-HYNIC in canine non-Hodgkin lymphoma. *PLoS One* 7(4):e34404
33. Beaino W, Nedrow JR, Anderson CJ (2015) Evaluation of ^{68}Ga - and ^{177}Lu -DOTA-PEG4-LLP2A for VLA-4-targeted PET imaging and treatment of metastatic melanoma. *Mol Pharm* 12(6):1929–1938
34. Choi J, Beaino W, Feczek RJ, Fabian KP, Laymon CM, Kurland BF, Storkus WJ, Anderson CJ (2018) Combined VLA-4-targeted radionuclide therapy and immunotherapy in a mouse model of melanoma. *J Nucl Med* 59(12):1843–1849
35. Koukouraki S, Strauss LG, Georgoulas V, Eisenhut M, Haberkorn U, Dimitrakopoulou-Strauss A (2006) Comparison of the pharmacokinetics of ^{68}Ga -DOTATOC and [^{18}F] FDG in patients with metastatic neuroendocrine tumours scheduled for ^{90}Y -DOTATOC therapy. *Eur J Nucl Med Mol Imaging* 33(10):1115–1122
36. Virgolini I, Ambrosini V, Bomanji JB, Baum RP, Fanti S, Gabriel M, Papathanasiou ND, Pepe G, Oyen W, De Cristoforo C (2010) Procedure guidelines for PET/CT tumour imaging with ^{68}Ga -DOTA-conjugated peptides: ^{68}Ga -DOTA-TOC, ^{68}Ga -DOTA-NOC, ^{68}Ga -DOTA-TATE. *Eur J Nucl Med Mol Imaging* 37(10):2004–2010
37. Haug A, Auernhammer CJ, Wängler B, Tiling R, Schmidt G, Göke B, Bartenstein P, Pöpperl G (2009) Intraindividual comparison of ^{68}Ga -DOTA-TATE and ^{18}F -DOPA PET in patients with well-differentiated metastatic neuroendocrine tumours. *Eur J Nucl Med Mol Imaging* 36(5):765–770
38. Prasad V, Ambrosini V, Hommann M, Hoersch D, Fanti S, Baum RP (2010) Detection of unknown primary neuroendocrine tumours (CUP-NET) using ^{68}Ga -DOTA-NOC receptor PET/CT. *Eur J Nucl Med Mol Imaging* 37(1):67
39. Gabriel M, Oberauer A, Dobrozemsky G, Decristoforo C, Putzer D, Kendler D, Uprimny C, Kovacs P, Bale R, Virgolini IJ (2009) ^{68}Ga -DOTA-Tyr3-octreotide PET for assessing response to somatostatin-receptor-mediated radionuclide therapy. *J Nucl Med* 50(9):1427
40. Hyduk SJ, Oh J, Xiao H, Chen M, Cybulsky MI (2004) Paxillin selectively associates with constitutive and chemoattractant-induced high-affinity $\alpha_4\beta_1$ integrins: implications for integrin signaling. *Blood* 104(9):2818–2824

Publisher's Note Springer Nature remains neutral with regard to jurisdictional claims in published maps and institutional affiliations.

Affiliations

Yongkang Gai^{1,2} · Lujie Yuan^{1,2} · Lingyi Sun³ · Huiling Li^{1,2} · Mengting Li^{1,2} · Hanyi Fang^{1,2} · Bouhari Altine^{1,2} · Qingyao Liu^{1,2} · Yongxue Zhang^{1,2} · Dexing Zeng³ · Xiaoli Lan^{1,2}

✉ Dexing Zeng
zengd@ohsu.edu

✉ Xiaoli Lan
LXL730724@hotmail.com

¹ Department of Nuclear Medicine, Union Hospital, Tongji Medical College, Huazhong University of Science and Technology, Wuhan 430022, China

² Hubei Province Key Laboratory of Molecular Imaging, Wuhan 430022, China

³ Center for Radiochemistry Research, Department of Diagnostic Radiology, Oregon Health and Science University, Portland, OR 97239, USA